Available online at www.sciencedirect.com

ScienceDirect

Procedia CIRP 46 (2016) 290 – 293

www.elsevier.com/locate/procedia

7th HPC 2016 – CIRP Conference on High Performance Cutting

Geometry optimization of polycrystalline diamond tools for the milling of sintered ZrO2

Maximilian Warhanek[a,*], Josquin Pfaff[a], Pablo Martin[a], Lukas Schönbächler[a], Jens Boos[b], Konrad Wegener[a,b]

[a]*Institute of Machine Tools and Manufacturing (IWF), ETH Zurich, Switzerland*
[b]*inspire AG for Mechatronic Production Systems and Manufacturing Technology, Switzerland*

* Corresponding author. Tel.: +41 44 633 78 40; fax: +41 44 632 11 59. *E-mail address:* warhanek@iwf.mavt.ethz.ch

Abstract

Recent developments on tangential ultrashort-pulsed laser processing enable the generation of solid polycrystalline diamond composite tools with increasing geometric flexibility. To exploit this potential, an experimental study on the influence of the tool geometry on the cutting characteristics and the tool wear while milling sintered Zirconia dioxide is conducted. Three different tool geometries and a variation in rake and flank angles are produced to investigate the effects on processing forces and tool lifetime. The results are applied to the design of an end mill achieving 1.2 mm³/mm s specific material removal rate over a tool lifetime of 8000 mm³/mm.

Peer-review under responsibility of the International Scientific Committee of 7th HPC 2016 in the person of the Conference Chair Prof. Matthias Putz

Keywords: Milling; Ceramic; Diamond Tool

1. Introduction

Processing of sintered industrial ceramics is conventionally performed by grinding with electroplated, brazed or vitrified bonded diamond tools. High tool wear, long processing times and the necessity of high-speed grinding spindles are the main challenges for this technology, when applied to geometries that require small diameter tools. High performance grinding processes for sintered Zirconia dioxide (ZrO_2), as presented by Rabiey et al. [1], achieve up to 8 mm³/mm s specific material removal rate using a novel hybrid-bonded diamond grinding tool with a diameter of 6 mm. New manufacturing technologies such as pulsed laser ablation (PLA) and electrical discharge machining (EDM) steadily increase the geometric freedom in the design of solid diamond tools. Accordingly, a number of recent publications investigate the possibility of manufacturing geometrically defined tools, mainly milling tools, from solid diamond materials. Yan et al. [2] use EDM with a rotary electrode for the generation of micro cutting features in polycrystalline diamond composite (PCD) tools. A similar approach is applied by Zhang et al. [3], who use wire EDM to produce micro PCD tools for the machining of tungsten carbide (WC). Cheng et al. [4] demonstrate the applicability of wire EDM to more complex tool geometries, including helical chip spaces and cutting edges. Suzuki et al. [5] produce mono-crystalline diamond tools by PLA. The tools are successfully applied to high-precision milling of WC molds. Butler-Smith et al. [6,7] achieve the production of a solid diamond micro-grinding tool with geometrically defined cutting edges and a PCD micro core drill by PLA.

A different approach to produce milling tools capable of cutting sintered ceramics is diamond coating of WC tools. On the one hand, this method has the drawback of significantly reducing tool lifetime, due to the additional wear mechanism of delamination [8]. On the other hand, it exhibits high geometric flexibility due to the more efficient shape-giving

Peer-review under responsibility of the International Scientific Committee of 7th HPC 2016 in the person of the Conference Chair Prof. Matthias Putz
doi:10.1016/j.procir.2016.04.003

processes on WC before the diamond coating is applied. Both these tools and similar tools applied in the work of Bian et al. [9] are used for milling sintered ZrO_2, giving insight into the geometric requirements of tools for this process. Based on these findings, this study examines the suitability of three distinctly different milling tool geometries for the processing of sintered ZrO_2 and investigates the influence of flank and clearance angles on the tool performance.

2. Tool design

Regarding the cutting parameters applied in the various studies mentioned in the introduction, chip thicknesses in the range from 0.18 to 5.28 µm are set for the milling of ZrO_2 and WC materials. These low values are chosen to achieve a ductile cutting mode, which according to Bifano et al. [10] requires a cutting depth below a material dependent critical value. Ductile cutting of hard materials is generally associated with better resulting surface quality on the workpiece. Furthermore, preliminary experiments reveal that low cutting depths are necessary while milling ceramic materials in order to limit the occurring process forces to avoid tool failure through overload breakage of the cutting edges or the entire tool shaft. Milling with chip thicknesses in this range does not require large chip spaces. Small chip spaces further have the advantage of allowing the arrangement of more cutting edges on the circumference of the tool, which in turn increases the lifetime of the tool. Based on this insight, the three tools designs, illustrated in Fig. 1, are established. For the sake of comparability, all three designs have a tool diameter of 1.9 mm and a chip space depth of 0.1 mm.

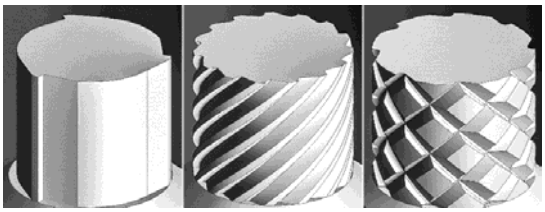

Fig. 1. Milling tool designs:
(left) geometry A; (middle) geometry B; (right) geometry C.

The design of geometry A is chosen for efficient investigation of the influence of rake and clearance angle variation on tool performance. For this purpose, three cutting edges are aligned parallel to the tool axis. This simplifies the manufacturing process and the measurement of the cutting edge geometry. Geometries B and C, are two distinctly different designs with helical cutting edges, generated for the purpose of investigating the influence of continuous and interrupted cutting edges on the tool performance. While geometry B constitutes a standard fluted milling tool, geometry C shall act similar to a micro-grinding tool with defined cutting edge geometries as presented in [6]. The number and size of the chip spaces is adjusted in a way that both tools have the same total cutting edge length. This results in milling tools with 15 helical cutting edges in case of geometry B and 8 rhombical cutting edges around the circumference of geometry C.

3. Experimental setups and test conditions

3.1. Measurement and performance evaluation

The produced tools are measured in the new state and at regular intervals during the milling experiments on an Alicona Infinite Focus 3D microscope. The 3D data allows for evaluation of cutting edge radii, surface roughness, clearance and rake angles as well as radial wear. The milling experiments to evaluate the performance of the different tool geometries are conducted on a high-precision 3-axes Mauser Präzoplan milling centre equipped with an Alfred Jäger type Z100-H536.05 spindle with 35'000 rpm. To investigate the development of the cutting efficiency over the lifetime of the tools, milling force measurements are performed during all experiments with a type 9257A Kistler 3-axes force measurement platform. The ZrO_2 material used for the milling experiments is supplied by METOXIT high tech ceramics. The material type TZP-A is stabilized with < 5 wt% Y_2O_3 and reinforced with < 0.25 wt% Al_2O_3. The hardness is specified as 1200 HV. Roughness measurements on milled surfaces are performed with a Taylor Hobson Form Talysurf 2 machine.

After preliminary experiments, the milling parameters are defined as summarized in Table 1. It is determined that the processing force levels of geometry C are approximately double of those of geometry B, when applied at the same parameters. It is concluded that geometry C acts as a tool with 8 teeth and the feed rate is reduced for this geometry to allow performance comparison with the same feed per tooth. All milling tests are performed without coolant or lubricant.

Table 1. Milling parameters.

Geometry	A	B / C
Cutting speed	50 m/min	50 m/min
Depth of cut (a_e)	0.1 mm	0.1 mm
Width of cut (a_p)	1 mm	1 mm
Feed rate	120 mm/min	720 / 384 mm/min
Spec. material removal rate	0.2 mm³/mm s	1.2 / 0.64 mm³/mm s
Strategy	parallel feed	parallel feed

3.2. Tool manufacturing

The tools are manufactured by ultrashort-pulsed laser ablation on a modified EWAG Laser Line machine tool. The high-precision machine is equipped with three linear stages in X', Y and Z' direction, two rotation stages in B' and C' configuration and three highly dynamic linear optical axes aligned parallel to the three linear axes. The laser system applied in this machine is a TimeBandwidth Fuego with a pulse duration of τ_P < 12 ps, an average power of P_{max} = 35 W and a pulse frequency range from 200 kHz to 8.2 MHz. The chip spaces of geometry A are produced by 2.5D volume ablation as described by Eberle et al. [11]. Supported by the CAM software Samlight SCAPS, this process gives the flexibility of efficient geometry adjustments for the variation of the rake angle. A final pass by tangential laser scanning is applied to set the clearance angle and sharpen the cutting edges while minimizing the circular runout of the tools. Geometries B and

C are generated by tangential laser processing as described in [12]. This process enables the uninterrupted processing of the circumferential chip spaces and allows for superior precision in terms of geometric repeatability and surface quality of the tools. Table 2 summarizes the laser parameters applied for both processes.

Table 2. Laser parameters.

Parameter	2.5D	Tangential
Wavelength	1064 nm	1064 nm
Beam quality M^2	< 1.3	< 1.3
Pulse duration	< 12 ps	< 12 ps
Fluence	0.86 J/cm²	6.1 J/cm²
Pulse frequency	672 kHz	800 kHz

The chosen PCD material for the tools is A3DP, supplied by Element Six. This PCD composite material has a diamond content of 93% with a grain size of 5 µm. As shown in Fig. 2, all three geometries are produced within reasonable tolerances by the mentioned laser processes. The considerable disadvantage regarding surface quality of the 2.5D process applied is clearly visible in the chip space of geometry A. Tangentially finished surfaces exhibit a surface roughness of Ra < 200 nm. Cutting-edge radii are measured in the range of 5.5 to 7.5 µm. A slight asymmetry of the cutting edges in geometry C could not be avoided, due to the different beam incidence conditions during the processing of the first and second helix direction.

Fig. 2. PCD Milling tools:
(left) Geometry A; (middle) Geometry B; (right) Geometry C.

4. Results and discussion

Four tools of geometry A with varying rake and clearance angles are tested. Fig. 3 illustrates the results of the tangential cutting force measurements. A considerable difference in the wear behaviour of the tools, measured by both the cutting force increase and radial wear, is determined between positive and negative rake angles. While the force levels of new tools are at the same level, the cutting forces increase significantly faster for tools with negative rake angle and the radial wear reaches the depth of the chip spaces after a short tool lifetime of 150 mm³/mm. The variation of clearance angles, however, does not significantly affect the wear behaviour in terms of cutting forces. Higher clearance angles decrease the cutting forces over the entire lifetime of the tools, but increase the occurrence of breakouts at the cutting edges.

The long-term tangential cutting forces of geometries B and C are compared in Fig. 4. The force levels of the new tools are higher than for geometry A, because of the higher amount of cutting edges, at least two of which are in contact with the workpiece at all times. In spite of the almost double material removal rate of geometry B, both tools operate at similar force levels during the first 500 mm³/mm of the tool lifetimes. After this stage, the cutting forces of geometry C increase at a slightly lower rate over the lifetimes of the tools. This is explained with the lower feed rate applied for geometry C while the total cutting edge length is similar to geometry B. It is assumed, that geometry B would perform at lower cutting forces and with less wear, if applied at the same feed rate. The radial wear measured during these tests after tool lifetimes of 2'500 mm³/mm is in the range of 6 and 12 µm on geometries B and C, respectively. Significant cutting-edge breakouts are observed only at the exposed edges at the tip of the tool. Considerable forces axial to the milling tools are measured during all experiments. These are caused by the lack of cutting edges on the face side of the cylindrical tools. Small amount of debris sticking to the rake faces are observed on all tested tools but not considered to have a significant effect on the cutting performance.

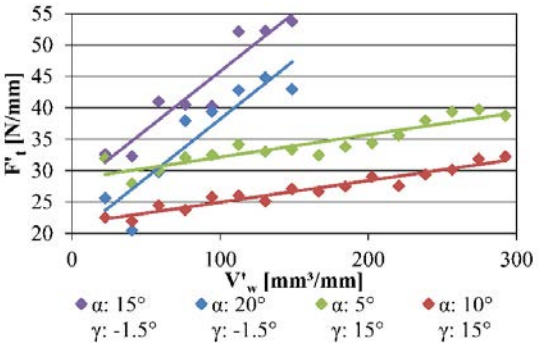

Fig. 3. Specific cutting forces with different clearance angles (α) and rake angles (γ).

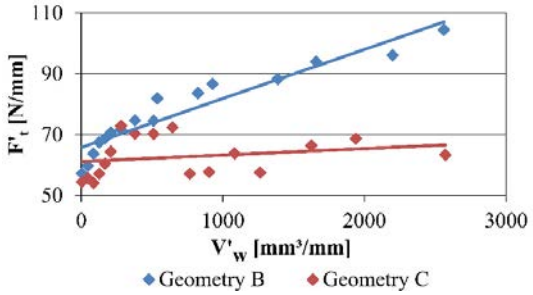

Fig. 4. Specific cutting forces with milling tool geometries B and C.

5. Optimized tool

Based on the findings an optimized tool design is defined. As the highest material removal to cutting force ratio could be achieved by geometry B, the single helix configuration is applied. Both rake and clearance angle are chosen at 5° to provide resistance against cutting-edge breakouts and radial wear. To protect the cutting edges near the tool tip a torus radius of 0.1 mm is added to the design. Finally, additional cutting edges are added on the face side of the tool. A hole in the middle of the face side provides constant incidence

condition for the tangential laser processing. The inner diameter is chosen geometrically to avoid damage at the cutting edges on the opposite side by the unfocussed laser beam. The resulting tool geometry, shown in Fig. 5, is produced entirely by tangential laser processing.

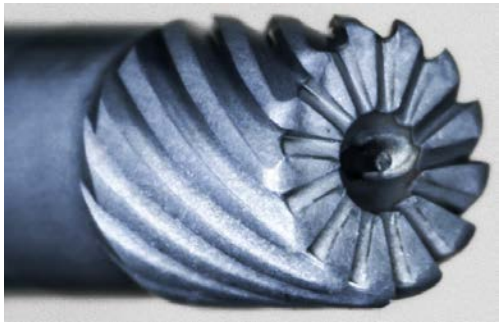

Fig. 5. PCD torus milling tool (diameter 1.8mm) with optimized geometry.

Tests with the optimized tool geometry show similar results with regards to cutting forces and wear behaviour as the tests with geometry B. The occurrence of cutting edge breakouts at the tool tip is reduced significantly by the torus radius. Further, milling experiments with the optimized tool and geometry B at high and low removal rates, as summarized in Table 3, are performed to investigate the capabilities of the tools for roughing and finishing processes.

Table 3. Roughing and finishing parameters.

Parameter	roughing	finishing
Cutting speed	50 m/min	68 m/min
Depth of cut (a_e)	0.1 mm	0.05 mm
Width of cut (a_p)	1 mm	1 mm
Feed rate	720 mm/min	200 mm/min
Spec. material removal rate	1.2 mm³/mm s	0.167 mm³/mm s
Strategy	parallel feed	parallel feed

Due to limitations of the processing forces caused by overload breakage at the threshold between PCD and WC Tool shaft, roughing removal rates cannot be increased above 1.2 mm³/mm s. At these parameters, a tool lifetime of 8080 mm³/mm is achieved. The surface measurements on the milled workpiece at the end of the tool lifetime show Ra values below 0.6 µm and Rz values below 3.5 µm (λc: 0.8 µm). These results are comparable with those achieved by high performance grinding with a 6 mm diameter tools in [1]. The roughness measurements on finished workpiece surfaces show Ra values below 25 nm and Rz values below 150 nm (λc: 0.25 µm).

6. Conclusions

Three different PCD tool geometries with axial, helical and cross-helical cutting edges are produced by ultrashort-pulsed laser ablation and evaluated by milling in sintered ZrO_2. The tangential laser process proves to be highly flexible with regards to the achievable tool geometries, especially when applied to features with small dimension. Significant differences in tool performance in terms of cutting forces and wear behaviour are observed and the findings are incorporated in an optimized tools design. As the tools are used without coolant or lubricant and with spindle speeds below 12’000 rpm, efficient applications are enabled compared to grinding tools of similar dimensions. The tools show promising results for both roughing and finishing applications. Compared to high performance grinding, lower material removal rates are achieved. However, similar tool life times and surface quality results are shown, in spite of the application of a three times lower tool diameter.

Future work will investigate the application of ultrashort-pulsed laser ablated PCD tools on other hard materials, such as Aluminium dioxide, glass and tungsten carbide.

Acknowledgements

The research leading to these results has received funding from the European Union Seventh Framework Programme (FP7/2007-2013) under grant agreement n° 314731. The authors gratefully thank EWAG AG and Diamoutils SAS for their contributions.

References

[1] Rabiey M, Jochum N, Kuster F. High performance grinding of zirconium oxide (ZrO2) using hybrid bond diamond tools. CIRP Annals. 2013;62:343-6

[2] Yan J, Watanabe K, Aoyama T. Micro-electrical discharge machining of polycrystalline diamond using rotary cupronickel electrode. CIRP Ann. 2014;63(1):209–12.

[3] Zhang Z, Peng H, Yan J. Micro-cutting characteristics of EDM fabricated high-precision polycrystalline diamond tools. Int J Mach Tools Manuf. 2013;65:99–106.

[4] Cheng X, Wang Z, Kobayashi S, Nakamoto K, Yamazaki K. Development of a computer assistant programming system for micro/nano milling tool fabrication by multi-axis wire EDM. Int J of Comput Integr Manuf. 2009;9:847–56.

[5] Suzuki H, Okada M, Fujii K, Matsui S, Yamagata Y. Development of micro milling tool made of single crystalline diamond for ceramic cutting. CIRP Ann. 2013;62(1):59–62.

[6] Butler-Smith P, Axinte D, Daine M. Solid diamond micro-grinding tools: From innovative design and fabrication to preliminary performance evaluation in Ti–6Al–4V. Int J Mach Tools Manuf. 2012;59:55–64.

[7] Butler-Smith P, Axinte D, Daine M, Kennedy A, Harper L, Bucourt J, et al. A study of an improved cutting mechanism of composite materials using novel design of diamond micro-core drills. Int J Mach Tools Manuf. 2015;88:175–83.

[8] Romanus H, Ferraris E, Bouquet J, Reynaerts D, Lauwers B. Micromilling of Sintered ZrO2 Ceramic via cBN and Diamond Coated Tools. Proc CIRP. 2014;14:371–6.

[9] Bian R, Ferraris E, He N, Reynaerts D. Process investigation on meso-scale hard milling of ZrO2 by diamond coated tools. Precis Eng. 2014;38(1):82–91.

[10] Bifano T, Dow T, Scattergood R. Ductile-regime grinding. A new technology for machining brittle materials. Trans ASME. 1991;113:184–9.

[11] Eberle G, Dold C, Wegener K. Laser fabrication of diamond micro cutting tool related geometries using a high-numerical aperture micro scanning system. Int J Adv Manuf Tech. 2015;81(5):1117-25

[12] Plüss C, Frei B, Dold C, Warhanek M, Walter C. Producing workpiece surface at workpiece using processing machine comprising laser with laser head and machine drive device. Patent DE201410109613 20140709, Sep 2014.